Of course, in a realistic experimental setting, this revival process will not go on forever, since the cavities C_1 and C_2 are subject to other sources of decoherence and dissipative effects such as photon loss on the mirror surfaces. It has been shown [254] that these processes would lead to an exponential decay of the amplitude of the revival peaks shown in Fig. 6.5, and thus it is unlikely that more than a few peaks could be observed in practice. Nonetheless, the observation of a single revival peak would already be an impressive experimental illustration of the fact that decoherence is, at least in principle, completely reversible.

6.2 Interferometry with C_{70} Molecules

In this section, we will describe a series of experiments carried out by the group of Anton Zeilinger at the University of Vienna. In essence, these experiments are a sophisticated version of the well-known double-slit experiment. However, instead of light or microscopic entities such as electrons, interference patterns are here observed for massive molecules. These experiments are remarkable for two reasons. First, they demonstrate the quantum "wave nature" of objects that would normally clearly fall into the "matter" category. Second, they show directly how the continuous action of decoherence gradually takes away the "quantumness" of these objects and transforms them into the familiar classical objects of our experience. Before we describe these experiments in more detail, let us first sketch in a few paragraphs a predecessor, namely, the double-slit experiment carried out with single electrons.

6.2.1 The Double-Slit Experiment with Electrons

When, in the year of 2002, the readers of *Physics World* were asked to nominate the "most beautiful experiment in physics" of all times, the winner turned out to be the double-slit experiment with single electrons [255]. Feynman had famously remarked [256] that the double-slit experiment is a phenomenon "which has in it the heart of quantum mechanics; in reality it contains the *only* mystery" of the theory. Indeed, it is probably difficult to fathom another experiment that embodies so simply and completely the strange features of quantum mechanics.

Interestingly, it was not until the year 1961 that the experiment in its original form—a double slit traversed by electrons—had actually been carried out by Claus Jönsson, a student of Gottfried Möllenstedt's at the University of Tübingen [257,258]. Möllenstedt had previously experimentally demonstrated electron interference using a different device, called the electron biprism—in essence, a very thin wire that splits the electron beam in half. This method bears similarities to the slip of paper the English scientist Thomas Young had

used at the beginning of the 19th century to split a beam of sunlight in experiments demonstrating the ability of light to exhibit wave-like constructive and destructive interference effects [259].

Perhaps even more surprising, the experiment that ensured that only a single electron was present in the apparatus at any time was carried out only in 1989 by Akira Tonomura and coworkers at Hitachi using an electron biprism, just as in Möllenstedt's experiments [260]. The resulting interference pattern is shown in Fig. 6.6. This experiment clearly reflects the "mysteries" of quantum mechanics, as it shows that the interference fringes are not induced by interactions between electrons, but are rather due to the wave nature of *individual* electrons. Decoherence in the electron-biprism interferometer was recently investigated by Sonnentag and Hasselbach [261], who studied the decay of the visibility of the interference pattern induced by Coulomb interactions between the electrons and a macroscopic and dissipative electron-gas and phonon-gas environment.

6.2.2 Experimental Setup

Let us now outline the experimental setup used by the Zeilinger group for demonstrating the wave nature of massive molecules. The original experiment, reported in 1999 in a *Nature* article by Markus Arndt and coworkers [262], used C_{60} molecules, often nicknamed "buckey balls" because of their shape (see Fig. 6.7). Subsequent experiments, results of which were first reported in a 2002 paper by the Zeilinger group [263], were carried out using even bigger C_{70} molecules (in the shape of an elongated buckey ball) and a different experimental setup [263–266]. Our following discussion will be based on this later series of experiments.

Let us first get a sense of how truly massive these C_{70} molecules are (relative to microscopic entities such as electrons, that is). Since each carbon
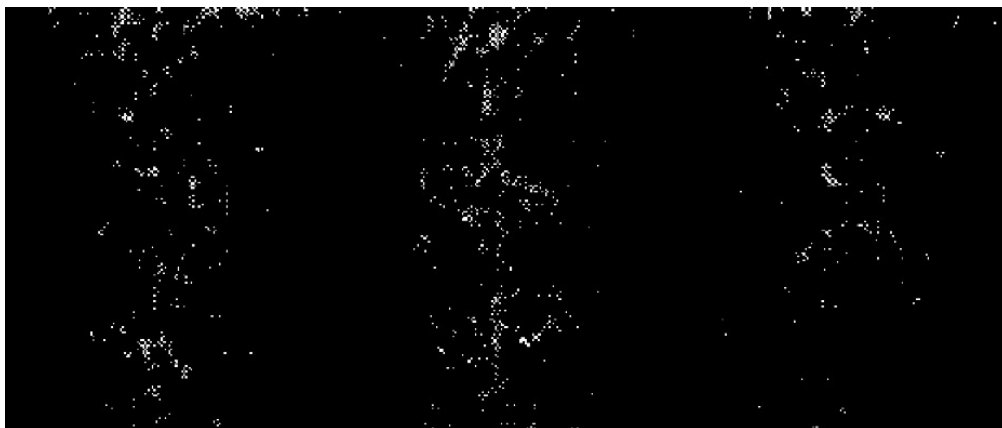

Fig. 6.6. Interference pattern from single electrons obtained in the double-slit experiment by Tonomura and coworkers [260]. Figure reprinted with permission from [260]. Copyright 1989 American Institute of Physics.
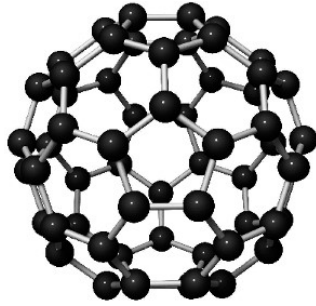
Fig. 6.7. Schematic illustration of a C_{60} molecule used in the original matter-wave interference experiment of Arndt et al. [262]. Sixty carbon atoms are arranged in the shape of a buckey ball with a diameter of about 1 nm.

atom contains six protons, six neutrons, and six electrons, a C_{70} molecule is composed of a total of over 1,000 microscopic constituents. Each such molecule possesses a very large number of highly excited internal rotational and vibrational degrees of freedom. This makes it possible to assign a finite temperature to each individual molecule. Also, emission of thermal radiation (i.e., of photons) from the molecules can be observed [266]. Thus, C_{70} molecules seem to clearly fall into the "particle" category.

Why is it so difficult to observe interference effects for such massive molecules? The relevant quantity is the matter de Broglie wavelength $\lambda = h/mv$, where m and v are the mass and velocity, respectively, of the particle. Thus the more massive and faster the particle, the shorter this wavelength. To observe interference effects with particles in a double slit–type experiment, the separation between the slits (and thus even more so the width of each slit) must be on the order of the wavelength. For typical velocities of C_{70} molecules in the experiment (around 100 m/s), the de Broglie wavelength of these molecules is a mere few picometers. The reader may easily imagine the impossibility of manufacturing such narrow, and narrowly spaced, slits.

How can this difficulty be overcome? The experiments of the Zeilinger group solve the problem through a neat trick that is based on the so-called *Talbot–Lau effect*. The basic principle of this effect is the following (see Fig. 6.8). Suppose a plane wave is traveling in the $+z$ direction, $f(z) = e^{2\pi i z/\lambda}$. Now we place a grating, composed of an array of parallel slits, at a right angle to the incoming wave. Let us denote the spacing of adjacent slits by d. One can then show (which we will not do here—see [267] for a short derivation) that at integer multiples of the distance

$$L_\lambda = \frac{d^2}{\lambda} \tag{6.29}$$

behind the grating the plane wave will in fact be *equal to the pattern of the grating.* In other words, if we place a screen at a distance nL_λ, $n = 1, 2, \ldots$, behind the grating and carry out the experiment with light, the screen will
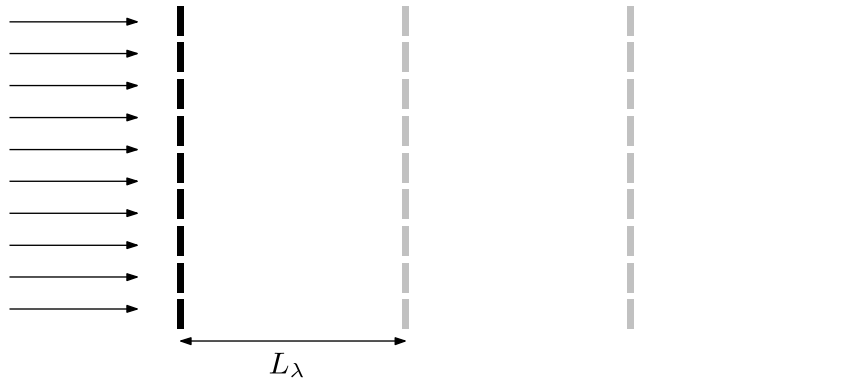
Fig. 6.8. Illustration of the Talbot–Lau effect. A plane wave traversing the grating on the left will generate an image of the grating at distances nL_λ, $n = 1, 2, \ldots$, from the grating.

show dark and light bands spaced a distance d apart, creating an image of the grating itself. This Talbot–Lau effect is a true interference phenomenon. Hence, if we carry out this experiment with matter particles and observe a density pattern equal to the grating pattern at multiples of the "Talbot length" L_λ, we have demonstrated the wave nature of these particles. To be sure, the fringes may in principle also be due to a simple blocking of rays by the grating (the so-called Moiré effect). However, the Moiré pattern is independent of the wavelength λ. Thus, to make sure that we actually deal with the Talbot–Lau effect, we can simply observe a variation in the pattern while varying λ. In the matter-wave case, this is achieved by changing the mean velocity v of the particles, since $\lambda = h/mv$.

A simple estimate will immediately convince the reader of the advantage of the Talbot–Lau method for detecting interference effects with C_{70} molecules. In the experiments of the Zeilinger group, the spacing d of the grating is about one micrometer, and the wavelength of the molecules equals a few picometer. Thus $L_\lambda \sim (10^{-6}\,\mathrm{m})^2/10^{-12}\,\mathrm{m} = 1\,\mathrm{m}$, i.e., all we need to do to observe the interference pattern is to place the "screen," i.e., a particle detector, at the macroscopic distance L_λ behind the grating. (The actual distance in the experiment is $L_\lambda = 38$ cm.) If we then measure a periodic variation of the particle density (with period d) that exhibits the characteristic wavelength dependence as we change the velocity of the molecules, we have confirmed the wave nature of these molecules.

The setup in the experiments of the Zeilinger group is schematically shown in Fig. 6.9. The C_{70} molecules are emitted from a source and then pass through a total of three identical free-standing gold gratings, each containing on the order of a thousand slits with period $d = 990\,\mathrm{nm}$. The purpose of the first grating is to induce a certain degree of coherence in the beam such that a diffraction pattern can be observed. The center grating acts as the actual diffraction grating. Finally, a third grating is placed at a distance equal to the
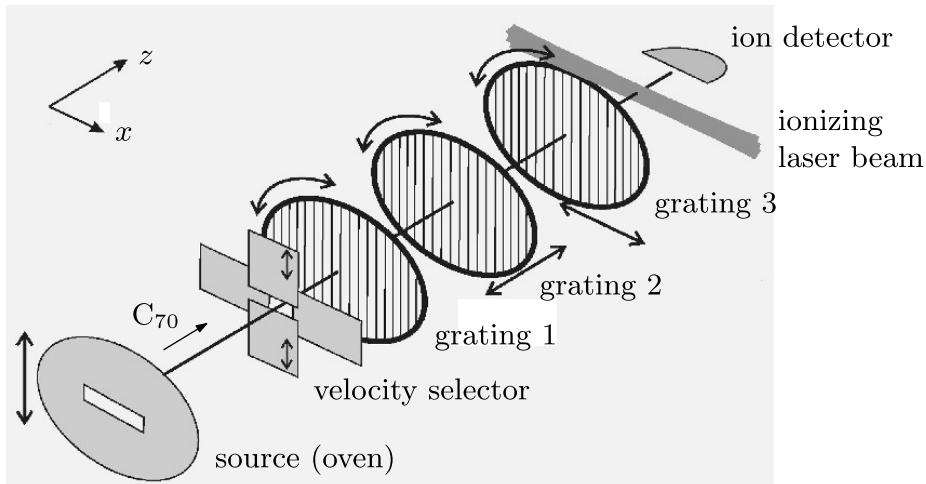
Fig. 6.9. Setup for observing matter-wave interference with C_{70} molecules in the experiments of the Zeilinger group [263–266]. Figure adapted with permission from [263]. Copyright 2002 by the American Physical Society.

Talbot length L_λ behind the diffraction grating. Recall that this means that, if the C_{70} molecules indeed possess a wave nature, an interference pattern will be obtained that, at the position of the third grating, will be an image of the diffraction grating itself. In other words, the molecular density would have periodic maximums and minimums along the x direction, with the peaks spaced apart by the slit spacing d. The purpose of the third grating is to act as a scanning mask for this molecular-density pattern. By moving the grating along x, the number of molecules registered behind the grating will fluctuate between a maximum and minimum value if an interference pattern is present. This fluctuation can then be easily measured by counting the number of molecules behind the third grating as a function of the x position of the grating.

The mean velocities of the molecules passing through the apparatus can be adjusted between about 90 m/s and 220 m/s by changing the position of the molecular source such that the fixed-height delimiter selects different portions of the beam, which follows a free-flight parabola. These velocities correspond to de Broglie wavelengths between 2 and 6 pm. The entire apparatus is contained in a vacuum chamber to minimize collisions between the C_{70} molecules and other particles.

6.2.3 Confirming the Wave Nature of Massive Molecules

The result of a typical run of the experiment is shown in Fig. 6.10. The horizontal axis corresponds to the position of the scanning mask along the x axis (see Fig. 6.9), and the vertical axis shows the molecular density behind the grating for each position. We clearly see the oscillatory fluctuations in the density of C_{70} molecules, which confirms the existence of spatial coherence
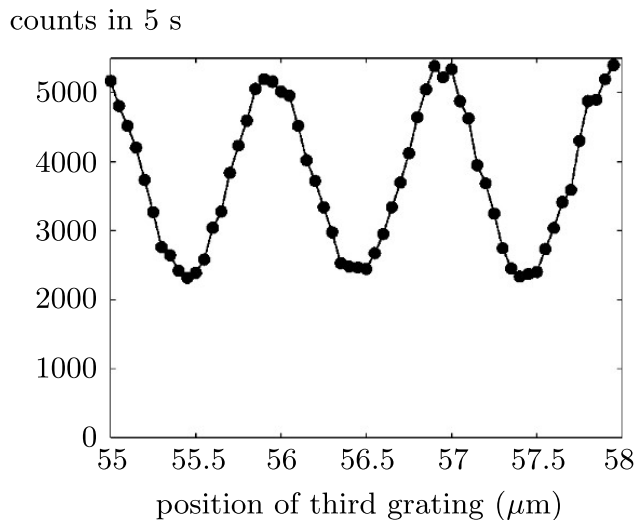
counts in 5 s

position of third grating (μm)

Fig. 6.10. Interference fringes for C_{70} molecules observed in the experiments of the Zeilinger group. The solid line is a fitted sine curve based on theoretical predictions. Figure adapted with permission from [263]. Copyright 2002 by the American Physical Society.

and interference effects. By varying the velocity of the molecules and observing the change in the density pattern (in agreement with the Talbot–Lau theory), it was also explicitly confirmed that this pattern is indeed due to the Talbot–Lau effect.

Also, the interference effect is a strict one-particle effect and not due to any interference between *different* molecules, for two reasons. First, interparticle interference would require that the interacting molecules are in the same state. However, since each C_{70} molecule has a very large number of internal degrees of freedom, the chances for this to be the case are effectively zero. Second, the distance between two molecules is much larger than the range of any intermolecular forces, so essentially only a single molecule is passing through the apparatus at any given time.

6.2.4 Which-Path Information and Decoherence

Let us now turn to the main theme of this chapter, namely, the experimental observation of decoherence. In the C_{70}-interference experiments, decoherence is dominantly due to collisions between C_{70} molecules and molecules in the background gas (which is always present in the apparatus to some degree, since the vacuum is never perfect). We described such collisional decoherence in detail in Chap. 3 and showed that it constitutes a ubiquitous source of decoherence in nature. However, as mentioned in the opening paragraphs of this chapter, for mesoscopic and macroscopic objects this decoherence is typically so fast as to make it effectively impossible to observe its gradual action.

This brings us to a key advantage of the C_{70}-interference experiments. Here, the amount of collisional decoherence can be precisely tuned by changing the density of the background gas. Fig. 6.11 displays the experimentally measured interference pattern for the C_{70} molecules for two different pressures (i.e., densities) of the background gas, as reported by Lucia Hackermüller et al. [267] (see also [264]). The left plot shows clearly visible interference fringes. As the pressure of the background gas is increased, the interference fringes become less pronounced (right plot). Let us quantify the visibility $V(p)$ of the interference pattern at a given background-gas pressure p as the relative difference between the maximum amplitude $c_{\mathrm{max}}(p)$ and minimum amplitude $c_{\mathrm{min}}(p)$ of the interference pattern,

$$V(p) = \frac{c_{\mathrm{max}}(p) - c_{\mathrm{min}}(p)}{c_{\mathrm{max}}(p) + c_{\mathrm{min}}(p)}. \tag{6.30}$$

In the idealized case of no decoherence and no other experimental imperfections, we would have $c_{\mathrm{min}} = 0$ and therefore full visibility. In the completely decohered case, no interference pattern would be observable and thus $c_{\mathrm{max}} = c_{\mathrm{min}}$, which implies zero visibility.

The experimental data [264, 267] for the change of the visibility (6.30) with gas pressure p is shown in Fig. 6.12. The visibility is found to decrease exponentially with p (note that the vertical axis is in logarithmic units). This exponential decay is in remarkable agreement with theoretical calculations [160, 268].
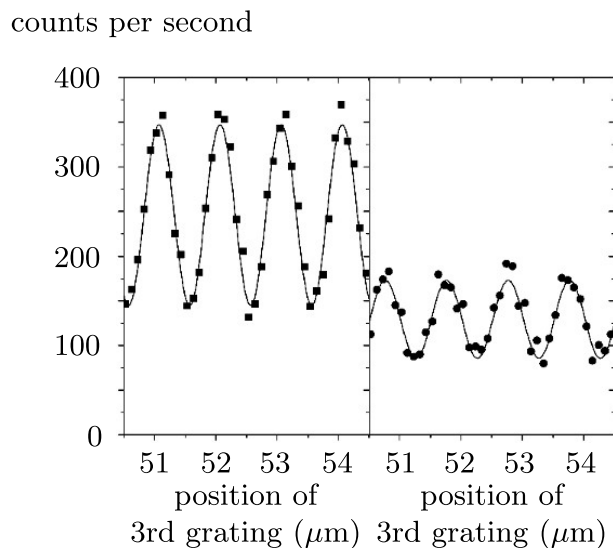

Fig. 6.11. Diminished interference effect in C_{70}-molecule interferometry due to decoherence induced by collisions with background-gas molecules, as observed in the experiments of the Zeilinger group [267]. The visibility of the interference fringes decreases when the pressure of the gas is increased from the left to the right panel. Figure adapted, with kind permission from Springer Science and Business Media, from [267].
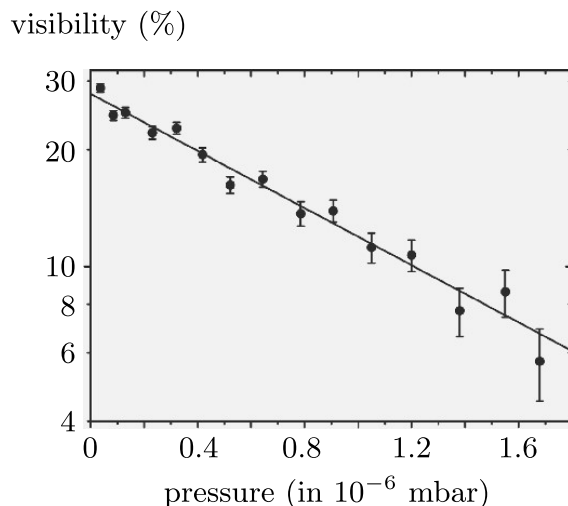
Fig. 6.12. Dependence of the visibility (6.30) of the interference pattern on the pressure of the background gas, as reported by the Zeilinger group [267]. The measured values (circles) are seen to agree well with the theoretical prediction (solid line), which describes an exponential decay of the visibility with pressure. Figure adapted, with kind permission from Springer Science and Business Media, from [267].

Thus these experiments provide impressive direct evidence for how the interaction with the environment gradually delocalizes the quantum coherence required for interference effects to be observed. This decoherence process occurs in a completely controlled way: By changing the amount of which-path information obtained by the environment (e.g., by altering the density of the background gas), the amount of decoherence and thus the loss of quantum features can be precisely tuned. So we can smoothly navigate and explore the quantum–classical boundary, and we find our observations to be in excellent agreement with theoretical predictions.

6.2.5 Decoherence Due to Emission of Thermal Radiation

What are the most important decoherence mechanisms for macroscopic bodies? Certainly, as we have seen, collisions with other particles (photons, air molecules, etc.) are ubiquitous and play a crucial role. However, another fundamental source of decoherence on these length scales is the emission of thermal radiation. Every "large" object is able to store energy in its many internal degrees of freedom. Macroscopic bodies essentially continuously absorb and emit photons. Each emitted photon carries away information about the path of the body, leading to decoherence in the position basis and therefore to spatial localization of the object.

For macroscopic objects, thermal emission of radiation is typically so strong as to completely preclude the possibility of observing spatial interference effects. Interestingly, as we shall see below, C_{70} molecules perfectly

navigate the boundary between the microscopic and macroscopic regimes with respect to thermal decoherence. They are small enough to allow for visible interference patterns to emerge, but they are also sufficiently complex that, when heated to a temperature of several thousand Kelvin, thermal decoherence leads to a complete disappearance of interference patterns. Thus these molecules are ideally suited for an explicit observation of thermal decoherence effects. All we need to do is to gradually heat up the molecules before they pass through the apparatus and then record the decay of the visibility of the interference fringes as a function of the molecular temperature.

This idea has been realized in a remarkable experiment that was carried out by members of the Zeilinger group and reported in 2004 by Hackermüller et al. [266]. Before passage through the gratings, the C_{70} molecules were heated by a laser beam from their source temperature of about 900 K to temperatures up to around 3,000 K. The observed interference pattern for four different values of laser power (and thus mean temperature of the molecules) is shown in Fig. 6.13.

We see that the visibility decreases with laser power due to thermal emission of radiation from the molecules, as expected. The results from a series of runs at various laser heating powers are shown in Fig. 6.14, and we observe that the experimental data is in good agreement with predictions obtained
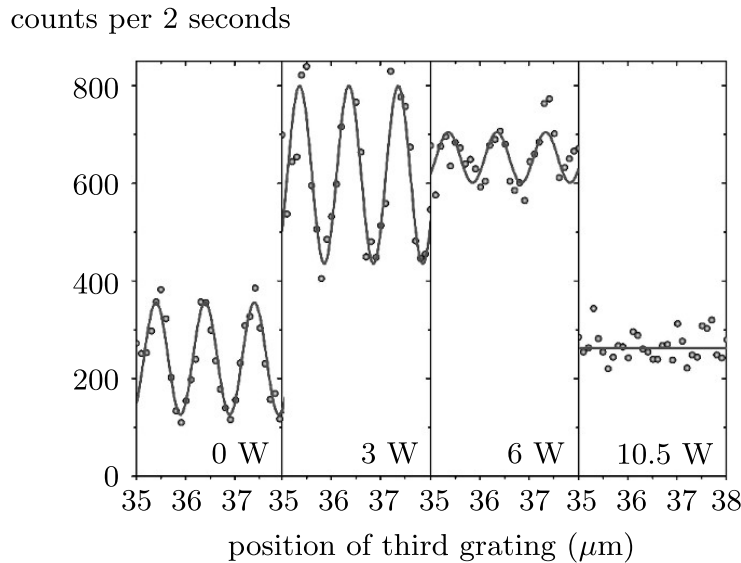

Fig. 6.13. Interference patterns for C_{70} molecules for different laser heating powers (inducing different mean temperatures of the molecules), as measured in the experiment by Hackermüller et al. [266]. The visibility of the interference fringes decreases as the average temperature of the molecules is increased. The variation in the overall average count rate at different values of laser heating power is due to variations of the efficiency of the ion-counting detector with the energy of the molecules and due to ionization and fragmentation effects in the heating stage. Figure reprinted from [266] by permission from Macmillan Publishers Ltd: Nature, copyright 2004.
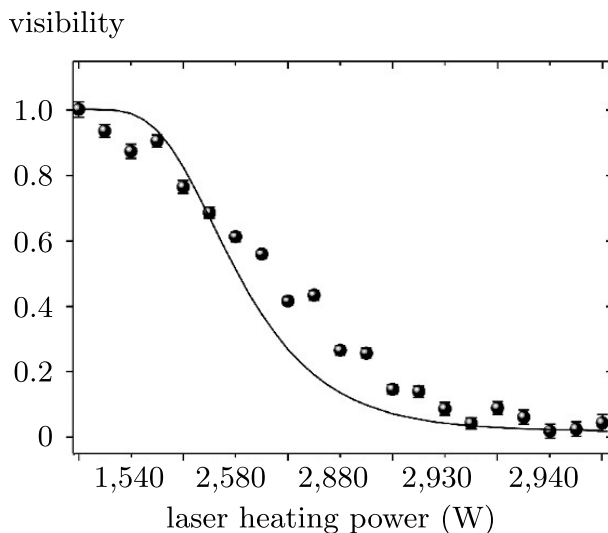
visibility

Fig. 6.14. Decay of the visibility of the C_{70} interference pattern as a function of laser heating power and mean molecular temperature in the experiment of Hackermüller et al. [266]. The circles represent experimental data, which agrees well with the theoretical prediction represented by the solid line. Figure reprinted from [266] by permission from Macmillan Publishers Ltd: Nature, copyright 2004.

from theoretical calculations [266]. A further detailed theoretical analysis of the experiment can be found in [269, 270].

The results demonstrate that for C_{70} molecules below temperatures of about 1,000 K, thermal decoherence is sufficiently weak for an interference pattern to be observed. At temperatures above about 2,000 K, thermal decoherence significantly reduces the visibility of the fringes, while around 3,000 K the interference pattern disappears completely.

This behavior can be explained as follows. For an emitted photon to transmit a sufficient amount of which-path information to resolve the path of the C_{70} molecule, its wavelength must be comparable to the separation of the different paths of the molecule, i.e., to the spacing between the maxima of the wave packets corresponding to passage of the molecule through the different slits in the diffraction grating. This separation is on the order of the spacing of the slits themselves, $d \approx 1 \, \mu m$, so thermal decoherence requires the emission of photons of wavelength $\lambda \lesssim 1 \, \mu m$. It turns out that only for temperatures above 2,000 K there is a significant probability of a C_{70} molecule to emit a photon of this wavelength. For temperatures around 3,000 K, the molecule typically emits several such photons. This transfers a sufficient amount of which-path information to the environment to entirely destroy the interference pattern.

6.2.6 Beyond Buckey Balls

Now that single-particle interference fringes have been experimentally observed for C_{70} molecules, we can naturally go further and attempt to demon-

strate such quantum effects for larger and larger molecules. In fact, the Zeilinger group has already taken the next step into this direction in an experiment reported by Hackermüller et al. in 2002 [265]. Using an experimental setup similar to that for C_{70} molecules, interference patterns were observed for the even more massive fluorinated fullerene $C_{60}F_{48}$ (mass $m = 1632$ amu, 108 atoms) and for the biomolecule tetraphenylporphyrin $C_{44}H_{30}N_4$ (mass $m = 614$ amu, width over 2 nm). The structure of these molecules is sketched in Fig. 6.15, and the resulting interference patterns are displayed in Fig. 6.16. Again, well-defined interference fringes are observed even for these comparably massive and complex molecules, and the measured visibilities were found to be in good agreement with theoretically predicted values.
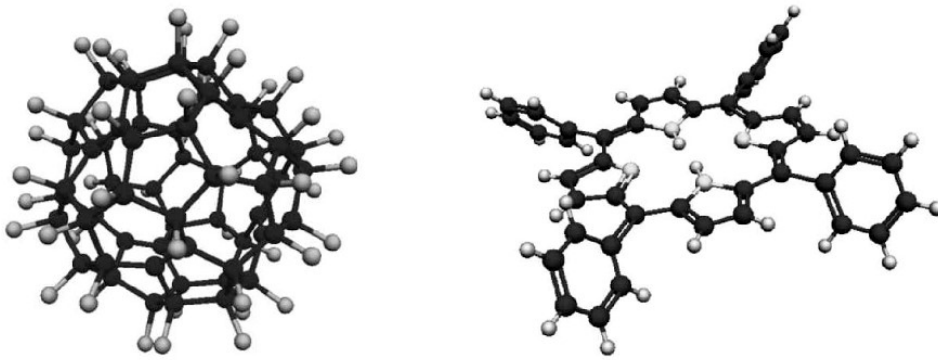

Fig. 6.15. Three-dimensional structure of the $C_{60}F_{48}$ molecule (left) and the biomolecule tetraphenylporphyrin $C_{44}H_{30}N_4$ (right) used in the interference experiments by Hackermüller et al. [265]. Figure reprinted with permission from [265]. Copyright 2003 by the American Physical Society.
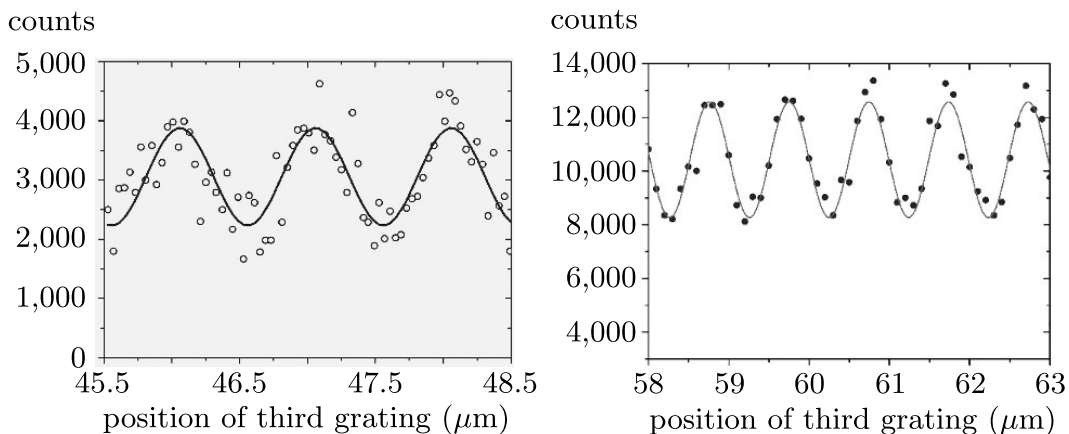

Fig. 6.16. Interference fringes for the $C_{60}F_{48}$ molecule (left) and the biomolecule tetraphenylporphyrin ($C_{44}H_{30}N_4$) (right) observed in the experiment by Hackermüller et al. [265]. The solid line is a fitted sine curve. Figure adapted with permission from [265]. Copyright 2003 by the American Physical Society.

One may now speculate about the feasibility of interference experiments that use even larger particles, for instance, biomolecules such as proteins and viruses [267, 271] or carbonaceous aerosols [270]. Such experiments will be limited by three main factors:

1. *Collisional decoherence.* In order to observe interference fringes for these molecules, the vacuum in the apparatus must be very good. Using a decoherence model for the visibility of interference fringes as a function of the density of the background gas, the quality of the vacuum in the apparatus required for the observation of interference effects has been estimated for several biomolecules up to the size of a rhinovirus [267,271] (see Fig. 6.17). The estimates assume the availability of an elongated Talbot–Lau interferometer with a spacing of one meter between the gratings (which is about three times more than the currently used distance), which has not yet been experimentally realized. Given this design, the required low background-gas densities are within the reach of current technology [264,267].

2. *Thermal decoherence.* This effect will become increasingly relevant on larger scales. For example, for a simple double-slit setup (as opposed to the Talbot–Lau interferometer) it has been estimated that a small virus (mass 5×10^7 amu) would need to be cooled down to about 40 K to exhibit a sufficiently visible interference pattern [270]. Obviously, it would be quite difficult to produce a beam of such "cold viruses" in the laboratory. For objects larger than the C$_{70}$ molecules, it may thus well turn out that
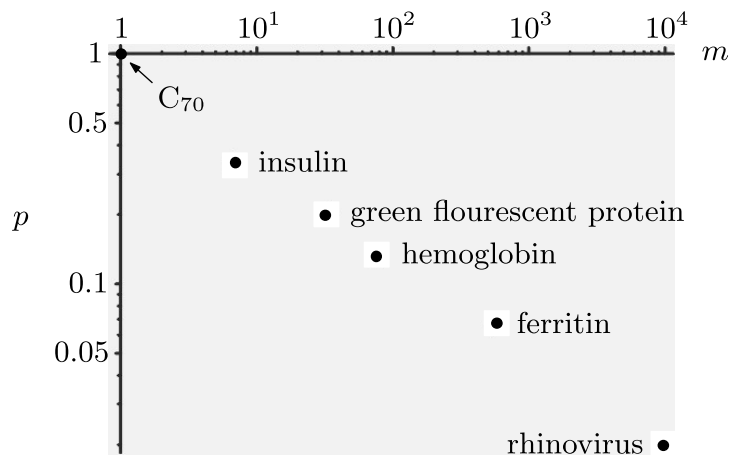

Fig. 6.17. Estimates for the maximum background-gas pressure p that would still permit the observation of interference fringes for several biomolecules in an elongated Talbot–Lau interferometer. The horizontal axis shows the molecular weight m relative to the mass of a C$_{70}$ molecule. The pressure, shown on the vertical axis, is normalized by the pressure required to observe interference with C$_{70}$ molecules. Plot generated using data reported by Hackermüller et al. [267].

it will be experimentally much more challenging to mitigate the effect of thermal decoherence than that of collisional decoherence [270].

3. *Dephasing due to inertial forces and vibrations.* While not a decoherence effect *per se*, the visibility of the interference pattern is also affected by noise due to gravitational, rotational, and acoustic perturbations, which are induced by the mass and rotation of the earth and by vibrations of the diffraction gratings [272]. These effects can severely limit the observability of the interference fringes, so the experimenters have taken much care to minimize these sources of noise in the Talbot–Lau setup described here. Still, for the particles listed in Fig. 6.17, vibrational noise is predicted to be a major obstacle to observing interference [272]. In currently available setups, this noise is likely to diminish the visibility of the interference pattern to a larger extent than collisional and thermal decoherence.

The important point to bear in mind is, however, that the conditions for an observation of interference effects can be precisely specified and quantified using theoretical decoherence models. We no longer have to limit ourselves to the assumption of a vaguely defined, fundamental divide between the quantum and classical realms as postulated by the Copenhagen interpretation. Instead, by treating the molecules of interest as open quantum systems interacting with their environments, we can understand what we need to do in order to observe interference effects, and why interference fringes are unobservable in a particular experimental setting.

The C_{70} molecules have the perfect amount of susceptibility to decoherence to allow for an observation of the gradual action of decoherence due to collisions with surrounding particles and due to the emission of thermal radiation. Thus it is difficult to imagine a more accessible and intuitive experiment for demonstrating the direct and controllable influence of decoherence that drives the system into the classical regime. It will be exciting to follow the development of research in this field, as future interference experiments are expected to push the envelope even further toward the macroscopic realm.

6.3 SQUIDs and Other Superconducting Qubits

Let us now turn to superconducting quantum two-state (qubit) systems. Over the past decade, these systems have become key players in experimental studies of macroscopic coherence and decoherence. They have gained additional importance as potential building blocks of superconducting quantum computers [273]. In the following, we shall focus on so-called superconducting quantum interference devices, or SQUIDs for short. We will also mention some related types of superconducting qubit systems such as Cooper-pair boxes.

A SQUID is a macroscopic quantum system that can exhibit a variety of fascinating quantum effects. In SQUIDs the state of billions of Bose-